Auger and radiative deexcitation of multiply ionized Ne†

Mau Hsiung Chen and Bernd Crasemann
Department of Physics, University of Oregon, Eugene, Oregon 97403
(Received 23 April 1975)

Radiative and Auger transition probabilities to the $1s$ state have been calculated for the individual multiplets of $Ne(1s)^1(2s)^j(2p)^k$ configurations. From multiplet fluorescence yields, the effective fluorescence yields $\bar{\omega}^i$ for Ne KL^i charge states were derived. For statistical distribution of multiplet states, we find $\bar{\omega}^i = 0.0159$, 0.0176, 0.0199, 0.0248, 0.0390, 0.0862, and 0.229 for $i = 0,\ldots,6$. These theoretical fluorescence yields agree well with experimental results from collisions of 30-MeV O^{5+} ions with Ne.

I. INTRODUCTION

Radiative and Auger decay rates of a $1s$ vacancy in Ne atoms containing i L-shell vacancies (charge states KL^i, $i = 0,\ldots,6$) have been calculated. From term transition rates, fluorescence yields were calculated for the individual multiplets LS that arise in a configuration n:

$$\omega(LS,n) = \frac{\Gamma_R(LS,n)}{\Gamma_R(LS,n) + \Gamma_A(LS,n)} \quad . \tag{1}$$

Here, Γ_R is the radiative width and Γ_A is the radiationless width of the decaying multiplet state.

The effective fluorescence yield of a given configuration is

$$\bar{\omega}(n) = \sum_{L,S} C_n(LS)\omega(LS,n), \tag{2}$$

where the $C_n(LS)$ are the population probabilities of multiplet states LS in the configuration n. For statistical population, we have

$$\bar{\omega}(n) = \sum_{L,S} (2L+1)(2S+1)\omega(LS,n) \times \left(\sum_{L,S}(2L+1)(2S+1)\right)^{-1}. \tag{3}$$

The effective fluorescence yield of a charge state i is

$$\bar{\omega}^i = \sum_n c_n \bar{\omega}(n), \tag{4}$$

where the summation extends over all possible configurations that belong to the given charge state i, and c_n is the population probability of configuration n in charge state i. For Ne charge states KL^i, the relevant electronic configurations are $(1s)^1(2s)^j(2p)^k$, $i = 8-j-k$.

The present approach, in which fluorescence yields for individual multiplet states are computed and subsequently averaged,[1,2] differs from the traditional *ansatz* in which radiative and total widths are separately averaged over all multiplet states.[3–5] The older approach led to large discrepancies between calculated x-ray and fluorescence yields and experimental data from ion-atom collisions, particularly for the higher charge states (Sec. VI). The present theoretical results, by contrast, appear to agree well with experiment.[6]

II. AUGER TRANSITION RATES

A. Initial vacancy configurations $[1s][2p]^n$

1. $[1s]^2S,[2p]^nL_4S_4; LS,\epsilon l_2; PQ \rightarrow [2s]^2S,[2p]^{n+1}P_4Q_4;$ *PQ transitions*

Formulas for the Auger decay rates of the pertinent multiplet states were derived from McGuire's general expressions for multiplet Auger transition rates in LS coupling.[7–9] The Auger rate for transitions between vacancy states indicated in the heading of this subsection (where ϵ and l_2 are the energy and angular momentum of the continuum electron) is

$$A(LS,PQ) = \frac{(n+1)(2P+1)(2Q+1)}{2L_4+1}\delta_{PP_4}\delta_{LL_4}\sum_{Q_4}(2Q_4+1)(p^{n+1}P_4Q_4\|p^nL_4S_4)^2 \times \left|\sum_f (-1)^f(2f+1)I(^{2f+1}P)\begin{Bmatrix} Q & f & S_4 \\ \frac{1}{2} & S & \frac{1}{2}\end{Bmatrix}\begin{Bmatrix} f & \frac{1}{2} & \frac{1}{2} \\ Q_4 & Q & S_4\end{Bmatrix}\right|^2 \tag{5}$$

in atomic units, where we have[2]

$$I(^1P) = -R_0(1s\epsilon p2s2p) - \tfrac{1}{3}R_1(1s\epsilon p2p2s), \quad I(^3P) = -R_0(1s\epsilon p2s2p) + \tfrac{1}{3}R_1(1s\epsilon p2p2s),$$

$$R_K(1s\epsilon p2s2p) = \int_0^\infty \int_0^\infty R_{1s}(r_1) R_{\epsilon p}(r_2) \frac{r_<^K}{r_>^{K+1}} R_{2s}(r_1) R_{2p}(r_2)\, dr_1\, dr_2. \tag{6}$$

2. $[1s]^2S,[2p]^nL_3S_3$; $LS,\epsilon l_2$; $PQ \rightarrow [2p]^{n+2}PQ$ transitions

The Auger rate for this type of transitions is

$$A(LS, PQ) = \frac{(n+1)(n+2)(2P+1)}{(2L+1)} \delta_{LL_3}\delta_{QS_3}\left[\tfrac{1}{6}R_1(1s\epsilon s2p2p)^2(p^{n+2}PQ \,\|\, p^2\,{}^1S;\, p^nL_3S_3)^2\right.$$

$$\left. + \tfrac{1}{15}R_1(1s\epsilon d2p2p)^2(p^{n+2}PQ \,\|\, p^2\,{}^1D;\, p^nL_3S_3)^2\right], \tag{7}$$

where

$$(p^{n+2}PQ \,\|\, p^2\,{}^1S;\, p^nL_3S_3)^2 = [6(2L_3+1)(2S_3+1)]^{-1}\delta_{L_3P}\left|\sum_{P',Q'}[(2P'+1)(2Q'+1)]^{1/2}(-1)^{P'+Q'}(p^{n+2}PQ \,\|\, p^{n+1}P'Q')(p^{n+1}P'Q' \,\|\, p^nL_3S_3)\right|^2 \tag{8}$$

and

$$(p^{n+2}PQ \,\|\, p^2\,{}^1D;\, p^nL_3S_3)^2 = \frac{5}{2(2S_3+1)}\left|\sum_{P'Q'}[(2P'+1)(2Q'+1)]^{1/2}(-1)^{Q'}\begin{Bmatrix} L_3 & 1 & P' \\ 1 & P & 2 \end{Bmatrix}(p^{n+2}PQ \,\|\, p^{n+1}P'Q')(p^{n+1}P'Q' \,\|\, p^nL_3S_3)\right|^2. \tag{9}$$

3. $[1s]^2S,[2p]^nL_RS_R$; $LS,\epsilon l_2$; $PQ \rightarrow [2s]^2\,{}^1S,[2p]^nL_RS_R$; PQ transitions

In these transitions, the active electrons originate from a closed shell. If one neglects the energy splitting caused by the presence of spectator holes, then the ordinary Auger transition-rate expressions are applicable.[10] The total rate is the same for all multiplets:

$$A = R_0(1s\epsilon s2s2s)^2. \tag{10}$$

B. Initial vacancy configurations $[1s][2s]^2[2p]^n$

The only possible Auger transitions from this configuration are $[1s]^2S, [2s]^2\,{}^1S$; ${}^2S, [2p]^nL_3S_3$; $LS, \epsilon l_2$; $PQ \rightarrow [2s]^2\,{}^1S, [2p]^{n+2}PQ$; PQ. Equations (7)–(9) can be used to find these multiplet Auger transition rates, because the empty $2s$ subshell has no effect on the calculation.

1. $[1s]^2S,[2p]^nL_3S_3$; $L_3S,[2s]^2S$; $L_iS_i,\epsilon l_2$; $PQ \rightarrow [2p]^{n+1}PQ,[2s]^2\,{}^1S$; PQ transitions

The Auger rate is

$$A[(L_3S)L_iS_i;\, PQ] = (2P+1)(2Q+1)(2S+1)(2L_3+1)^{-1}\delta_{L_iL_3} \times |(n+1)^{1/2}(p^{n+1}PQ \,\|\, p^nL_3S_3)\{(2S_3+1)^{-1}R_0(1s\epsilon p2s2p)\delta_{S_iS_3} - (-1)^{S_i-S_3}[3(2S+1)]^{-1}R_1(1s\epsilon p2p2s)]\delta_{QS}\}|^2. \tag{11}$$

C. Initial vacancy configurations $[1s][2s][2p]^n$

Some of the initial LS terms occur more than once in these configurations. For such multiplet states, mixing of the parent-ion states is included in the calculation. The mixing coefficients are found by diagonalizing the energy matrix.[11] If pure parent-ion states are assumed, then the wave functions and transition probabilities for multiplets occurring more than once will depend upon the way in which the parent ions are chosen. However, the energy eigenstates are independent of the order of coupling of the three open shells.[11] We couple the initial configuration as $[1s]^2S, [2p]^nL_4S_4$; $LS, [2s]^2S$; L_iS_i, in order to take advantage of existing information on electrostatic-interaction[11] and x-ray transition[12] matrix elements.

2.[1s] ^2S,[2p]$^n L_3S_3$; L_3S,[2s] ^2S; $L_iS_i,\epsilon l_2$; $PQ \rightarrow$ [2p]$^{n+2}P_3Q_3$,[2s] ^2S; PQ transitions

For the Auger transition rate, we have

$$A[(L_3S)L_iS_i,(P_3Q_3)PQ]=\frac{(2P+1)(2Q+1)(2S+1)}{3(2L_3+1)}(n+1)(n+2)\begin{Bmatrix}\frac{1}{2} & S_3 & S\\ \frac{1}{2} & S_i & Q\end{Bmatrix}^2\delta_{P_3P}\delta_{L_iL_3}\delta_{S_3Q_3}$$
$$\times[\tfrac{1}{2}(p^{n+2}P_3Q_3\,\|\,p^2\,{}^1S;\,p^nL_3S_3)^2R_1(1s\epsilon s2p2p)^2+\tfrac{1}{25}(p^{n+2}P_3Q_3\,\|\,p^2\,{}^1D;\,p^nL_3S_3)^2R_1(1s\epsilon d2p2p)^2]. \tag{12}$$

If the energy splitting between multiplet states is neglected, we can sum over P, Q:

$$A[(L_3S)L_iS_i,\,P_3Q_3]=[3(2L_3+1)]^{-1}(2P_3+1)(n+1)(n+2)\delta_{L_iL_3}\delta_{S_3Q_3}$$
$$\times\{\tfrac{1}{2}(p^{n+2}P_3Q_3\,\|\,p^2\,{}^1S;\,p^nL_3S_3)^2R_1(1s\epsilon s2p2p)^2+\tfrac{1}{25}(p^{n+2}P_3Q_3\,\|\,p^2\,{}^1D;\,p^nL_3S_3)^2R_1(1s\epsilon d2p2p)^2\}. \tag{13}$$

One can see that all the $A[(L_3S)L_iS_i,\,P_3Q_3]$ are independent of S_i and S.

If mixing of parent terms is included, we find

$$A_m[(L_3S)'L_iS_i,\,P_3Q_3)PQ]=[3(2L_3+1)]^{-1}(2P+1)(2Q+1)(n+1)(n+2)\delta_{P_3P}\delta_{L_iL_3}\delta_{S_3Q_3}$$
$$\times\left|\sum_S(-1)^\delta C(L_3S,\,L_iS_i)(2S+1)^{1/2}\begin{Bmatrix}\frac{1}{2} & S_3 & S\\ \frac{1}{2} & S_i & Q\end{Bmatrix}\right|^2F^2, \tag{14}$$

where the $C(L_3S,\,L_iS_i)$ are the mixing parameters, δ is the phase factor, and F is the quantity in curly brackets on the right-hand side of Eq. (13).

We have

$$A_m[(L_3S)'L_iS_i,\,P_3Q_3]=\sum_{P,Q}A_m[(L_3S)'L_iS_i,\,(P_3Q_3)PQ]=\sum_S C(L_3S,\,L_iS_i)^2A[(L_3S)L_3S_i,\,P_3Q_3]. \tag{15}$$

Because $A[(L_3S)L_3S_i,\,P_3Q_3]$ is independent of S, and the sum $\sum_S C(L_3S,\,L_iS_i)^2$ is equal to unity, the relation

$$A_m[(L_3S)'L_iS_i,\,P_3Q_3]=A[(L_3S)L_3S_i,\,P_3Q_3] \tag{16}$$

follows; including the mixing of parent terms does not change the rates for transitions of this type.

III. THE MULTIPLET X-RAY TRANSITION RATES

The x-ray transition rates were calculated in dipole approximation, in LS coupling, following the approach of Shore and Menzel.[12]

A. $(1s)^2S,(2p)^n(S_3L')$; $S'L'J'\rightarrow(1s)^2\,{}^1S,(2p)^{n-1}(SL)$; SLJ transitions

The x-ray emission rate is given by

$$(2J'+1)R(\alpha'S'L'J',\,\alpha SLJ)=\tfrac{4}{3}k^3S(\alpha'S'L'J',\,\alpha S'L\,J)\delta_{SS'}, \tag{17}$$

where we have

$$S^{1/2}=(-1)^{S'+J+L+1}[(2J+1)(2S'+1)]^{1/2}\sqrt{n}(p^{n-1}S'L\,\|\,p^nS_3L')\left(\frac{2S_3+1}{2S'+1}\right)^{1/2}\left(\frac{2L'+1}{3}\right)^{1/2}\begin{Bmatrix}S' & J & L\\ 1 & L' & J'\end{Bmatrix}g(s-p) \tag{18}$$

and

$$g(s-p)=-\int P_{1s}(r)rP_{2p}(r)\,dr. \tag{19}$$

The rate is in atomic units if the wave number k is

$$k=(E_i-E_f)/27.21c, \tag{20}$$

with E in electron volts.

If the energy splitting between multiplet states is neglected, then the total transition rate for each $L'S'$

state is

$$R(\alpha' S' L') = \sum_{L,S} \sum_{J,J'} \frac{(2J'+1) R(\alpha' S' L' J', \alpha S L J)}{(2L'+1)(2S'+1)} = \tfrac{4}{3} k^3 \frac{2S_3+1}{3(2S'+1)} \sum_L n(p^{n-1} S' L \,\|\, p^n S_3 L')^2 g(s-p)^2. \tag{21}$$

B. $(1s)^2 S, (2p)^n S_3 L'; \bar{S}_2 L', (2s)^2 S; S'L'J' \rightarrow (1s)^2\, {}^1S, (2p)^{n-1} S_1 L; S_1 L, (2s)^2 S; SLJ$ transitions

For transitions of this class, the x-ray emission rate is given by

$$(2J'+1) R(\alpha' S' L' J', \alpha S L J) = \tfrac{4}{3} k^3 S(\alpha' S' L' J', \alpha S' L J) \delta_{SS'}, \tag{22}$$

where

$$S^{1/2} = (-1)^{S'+J+L+1} [(2J+1)(2J'+1)]^{1/2} \begin{Bmatrix} S' & J & L \\ 1 & L' & J' \end{Bmatrix} \delta_{S_1 S_2} \sqrt{n} (p^{n-1} S_1 L \,\|\, p^n S_3 L') \left(\frac{2S_3+1}{2S_2+1}\right)^{1/2} \left(\frac{2L'+1}{3}\right)^{1/2} g(s-p) \tag{23}$$

and

$$R(\alpha' S' L') = \sum_{L,S} \sum_{J,J'} \frac{(2J'+1) R(\alpha' S' L' J', \alpha S L J)}{(2L'+1)(2S'+1)} = \tfrac{4}{3} k^3 \frac{2S_3+1}{3(2S_2+1)} \sum_L n(p^{n-1} S_1 L \,\|\, p^n S_3 L') \delta_{S_1 S_2} g(s-p)^2. \tag{24}$$

IV. THE SPIN-ORBIT INTERACTION MATRIX ELEMENTS FOR THE $(1s)^1 (2s)^1 (2p)^n$ CONFIGURATION

The matrix elements of the spin-orbit interaction for sp^n configurations were taken from Condon and Shortley[13]; those for $sp^n s'$ configurations were evaluated following the procedure of Wybourne, [14] through which the following expression can be derived:

$$\langle (1s)^2 S, (2p)^n S_1 L;\ S_2 L, (2s)^2 S;\ SLJM | H_{SO} | (1s)^2 S, (2p)^n S_1' L';\ S_2' L', (2s)^2 S;\ S'L'J'M \rangle$$

$$= (-1)^{\delta} [(2S+1)(2S'+1)(2S_2+1)(2S_2'+1)]^{1/2} \begin{Bmatrix} S & S' & 1 \\ L' & L & J \end{Bmatrix} \begin{Bmatrix} S & S' & 1 \\ S_2' & S_2 & \frac{1}{2} \end{Bmatrix} \begin{Bmatrix} S_2 & S_2' & 1 \\ S_1' & S_1 & \frac{1}{2} \end{Bmatrix} \sqrt{6} (p^n S_1 L \,\|V^{(11)}\|\, p^n S_1' L') \zeta_{2p}, \tag{25}$$

where

$$(p^n S_1 L \,\|V^{(11)}\|\, p^n S_1' L') = n(3/2)^{1/2} [(2S_1+1)(2L+1)(2S_1'+1)(2L'+1)]^{1/2}$$

$$\times \sum_{\bar{L},\bar{S}} (p^n S_1 L \,\|\, p^{n-1}(\overline{SL})(p^{n-1}\overline{SL} \,\|\, p^n S_1' L') \begin{Bmatrix} S_1 & S_1' & 1 \\ \frac{1}{2} & \frac{1}{2} & \bar{S} \end{Bmatrix} \begin{Bmatrix} L & L' & 1 \\ 1 & 1 & \bar{L} \end{Bmatrix} (-1)^{\bar{S}+\bar{L}+S_1+L-1/2} \tag{26}$$

and

$$\delta = J + 2S' + 2S_1 + L + S_1'. \tag{27}$$

V. NUMERICAL CALCULATIONS

A. Atomic model

The Herman-Skillman[15] Hartree-Slater model with Xα exchange potential was used in these calculations to generate the wave functions needed for computing the Auger and x-ray radial matrix elements.[16] The single-particle wave functions for each ion state were evaluated in the appropriate self-consistent-field (SCF) potential for that state. The neutral-atom exchange parameter[17] α was used for all ionization states.

B. Auger and x-ray energies

Average Auger and x-ray energies were used for all multiplet transition-rate calculations. In Ne, the typical Auger energy is ~700 eV and the typical x-ray energy ~850 eV. Neglecting multiplet energy splitting implies an error of <10 eV; this error affects the Auger transition rates by <2% and the x-ray transition rates by <3%.

The average energies for the $(1s)^1(2s)^2(2p)^n$ configurations were taken from Larkins' adiabatic Hartree-Fock calculations.[18] Energies for $(1s)^1(2s)^1(2p)^n$ configurations were derived from

TABLE I. Auger and x-ray transition probabilities (in multiples of 10^{-4} a.u.) to the K shell for initial $(1s)^1(2s)^2(2p)^n$ configurations of Ne, multiplet fluorescence yields $\omega(LS)$, and effective configuration fluorescence yields $\bar{\omega}(n)$ (calculated for statistical population).

		Auger transition probability				X-ray transition		
n	Multiplet	K-L_1L_1	K-L_1L_{23}	K-$L_{23}L_{23}$	Total	probability	$\omega(LS)$	$\bar{\omega}(n)$
6	^2S	8.366	25.12	58.61	92.10	1.489	0.0159	0.0159
5	^1P	9.472	19.773	48.026	77.271	2.219	0.0279	0.0168
	^3P	9.472	26.357	48.026	83.855	1.109	0.0131	
4	^2S	10.815	23.193	35.498	69.506	1.237	0.0175	0.0185
	^2P	10.815	15.472	29.192	55.479	2.475	0.0427	
	^4P	10.815	27.053	29.192	67.060	0.619	0.009 15	
	^2D	10.815	23.193	45.446	79.454	1.237	0.0153	
3	^3S	12.379	9.040	0	21.419	2.747	0.114	0.0229
	^5S	12.379	27.027	0	39.406	0	0	
	^1P	12.379	13.537	21.275	47.191	2.060	0.0418	
	^3P	12.379	22.530	21.275	56.184	0.687	0.0121	
	^1D	12.379	13.537	29.122	55.038	2.060	0.0360	
	^3D	12.379	22.530	29.122	64.031	0.687	0.0106	
2	^2S	14.055	15.642	9.112	38.809	0.760	0.0192	0.0272
	^2P	14.055	5.254	0	19.309	2.280	0.106	
	^4P	14.055	20.836	0	34.891	0	0	
	^2D	14.055	15.642	22.780	52.477	0.760	0.0143	
1	^1P	15.742	0.0549	•••	15.796	1.672	0.0957	0.0239
	^3P	15.742	11.856	•••	27.597	0	0	

the work of Matthews,[19] and those for $(1s)^1(2s)^0(2p)^n$ configurations, from the Hartree-Fock-Slater calculations of Bhalla *et al.*[5] In fact, the energy difference between a $2s$ hole and a $2p$ hole is virtually negligible, being of the same order as the multiplet splitting within a single configuration.

C. Calculation of multiplet Auger and x-ray transition rates

Auger and x-ray transition rates were computed in LS coupling from expressions derived in Secs. II and III (Tables I–III). In the $(1s)^1(2s)^1(2p)^n$ configurations, some of the multiplets occur more than once. In these cases, the mixing of parent terms was included.[11] The electrostatic-interaction matrix elements were taken from Slater's work.[11] Numerical values of the Slater integrals were calculated in the present atomic model (Table IV).

The initial configurations $(1s)^1(2p)^3$, $(1s)^1(2p)^2$, $(1s)^1(2s)^1(2p)^2$, and $(1s)^1(2s)^1(2p)^1$ contain some multiplet states for which Auger or x-ray decay channels are closed in LS coupling. For these multiplets, the initial states were expressed in intermediate coupling. The final states, however, were expressed in LS coupling, because after Auger transitions the final states contain only one multiplet. It has been shown by McGuire[20] that, if the initial state is expressed in intermediate coupling and the final state in LS coupling, then there is no interference and the Auger transition rate can be written as a linear combination of transition rates in LS coupling:

$$A(LSJ, PQ) = \sum_{L,S} C(LSJ)^2 A(LS, PQ). \tag{28}$$

The mixing parameters $C(LSJ)$ in the intermediate coupling scheme were obtained by diagonalizing the energy matrx. The matrix elements of the spin-orbit interaction for sp^n configurations were taken from Condon and Shortley,[13] and those for sp^ns' configurations were evaluated through the expressions derived in Sec. IV. The matrix elements of electrostatic interaction were taken from Slater's work.[11] The calculated spin-orbit parameters ζ_{nl} are included in Table IV.

VI. RESULTS AND DISCUSSION

Auger and x-ray transition probabilities, as well as fluorescence yields $\omega(LS, n)$, are listed in Tables I–III for all initial multiplet states pertaining to the configurations $(1s)^1(2s)^2(2p)^n$, $(1s)^1(2s)^1(2p)^n$, and $(1s)^1(2s)^0(2p)^n$. Effective fluo-

TABLE II. Auger and x-ray transition probabilities (in multiples of 10^{-4} a.u.) to the K shell for initial $(1s)^1(2s)^1(2p)^n$ configurations of Ne, multiplet fluorescence yields $\omega(LS)$, and effective configuration fluorescence yields $\bar{\omega}(n)$ (calculated for statistical population).

n	Multiplet	Auger transition probability K-L_1L_{23}	Auger transition probability K-$L_{23}L_{23}$	Auger transition probability Total	X-ray transition probability	$\omega(LS)$	$\bar{\omega}(n)$
6	^1S	42.990	70.639	113.629	1.644	0.0143	0.0196
	^3S	5.029	70.639	75.668	1.644	0.0213	
5	$(^1P)^2P'$	22.667	53.548	76.215	2.227	0.0284	0.0215
	$(^3P)^2P'$	25.171	53.548	78.719	1.346	0.0168	
	$(^3P)^4P$	4.042	53.548	57.59	1.191	0.0203	
4	$(^2S)^1S$	38.079	38.920	76.999	1.315	0.0168	0.0260
	$(^2S)^3S$	4.751	38.920	43.671	1.315	0.0292	
	$(^4P)^5P$	2.375	31.942	34.317	0.658	0.0188	
	$(^4P)^3P'$	30.421	31.942	62.363	0.754	0.0119	
	$(^2P)^1P$	9.501	31.942	41.443	2.631	0.0595	
	$(^2P)^3P'$	14.785	31.942	46.727	2.536	0.0513	
	$(^2D)^1D$	38.079	49.711	87.790	1.315	0.0147	
	$(^2D)^3D$	4.751	49.711	54.462	1.315	0.0235	
3	$(^5S)^6S$	2.345×10^{-4}	1.926×10^{-3}	2.161×10^{-3}	6.318×10^{-5}	0.0284	0.0459
	$(^5S)^4S'$	33.946	0	33.946	0.0879	0.002 58	
	$(^3S)^4S'$	6.092	0	6.092	2.912	0.323	
	$(^3S)^2S$	11.149	0	11.149	3.003	0.212	
	$(^1P)^2P'$	15.987	22.897	38.884	2.063	0.0504	
	$(^3P)^2P'$	23.976	22.897	46.873	0.940	0.0197	
	$(^3P)^4P$	2.787	22.897	25.684	0.751	0.0284	
	$(^1D)^2D'$	15.987	31.252	47.239	2.063	0.0418	
	$(^3D)^4D$	2.787	31.252	34.039	0.751	0.0216	
	$(^3D)^2D'$	24.053	31.252	55.305	0.940	0.0167	
2	$(^2S)^1S$	24.808	9.653	34.461	0.830	0.0235	0.0855
	$(^2S)^3S$	3.262	9.653	12.915	0.830	0.0604	
	$(^4P)^5P'_3$	2.455×10^{-4}	1.812×10^{-3}	2.058×10^{-3}	6.246×10^{-5}	0.0295	
	$(^4P)^5P'_2$	7.917×10^{-5}	4.386×10^{-4}	5.178×10^{-4}	1.291×10^{-5}	0.0243	
	$(^4P)^5P'_1$	2.677×10^{-4}	7.869×10^{-4}	10.544×10^{-4}	8.818×10^{-5}	0.0772	
	$(^4P)^3P'$	27.225	0	27.225	0.1281	0.00468	
	$(^2P)^1P$	9.785	0	9.785	2.490	0.203	
	$(^2P)^3P'$	4.296	0	4.296	2.362	0.355	
	$(^2P)^1D$	24.808	24.078	48.886	0.830	0.0167	
	$(^2D)^3D$	3.262	24.078	27.340	0.830	0.0295	
1	$(^1P)^2P'$	1.687	···	1.687	1.611	0.488	0.237
	$(^3P)^2P'$	17.703	···	17.703	0.213	0.0119	
	$(^3P)^4P'_{1/2}$	8.323×10^{-5}	···	8.323×10^{-5}	6.380×10^{-5}	0.434	
	$(^3P)^4P'_{3/2}$	2.165×10^{-4}	···	2.165×10^{-4}	1.629×10^{-4}	0.429	
	$(^3P)^4P^o_{5/2}$	2.824×10^{-5}	···	2.824×10^{-5}	5.370×10^{-7}	0.0187 [a]	

[a] The $^4P^o_{5/2}$ rates are from Ref. 21.

rescence yields $\bar{\omega}(n)$ for each configuration are also listed. In Table V, we indicate the possible configurations for each charge state KL^i, the fluorescence yields $\bar{\omega}(n)$ and weights of the configurations, and the effective fluorescence yields $\bar{\omega}^i$ of the charge states, computed according to Eq. (4).

The configuration fluorescence yields $\bar{\omega}(n)$, calculated in accordance with Eq. (3), can differ substantially from results derived through the (erroneous) old averaging procedure

$$\bar{\omega}(n)=\frac{\Gamma_R}{\Gamma_R+\Gamma_A}=\frac{\sum_{L,S}(2L+1)(2S+1)\Gamma_R(LS,n)}{\sum_{L,S}(2L+1)(2S+1)[\Gamma_R(LS,n)+\Gamma_A(LS,n)]}. \tag{29}$$

For low ionization states, the old and new approaches give similar results, because the Auger widths $\Gamma_A(LS,n)$ are nearly equal for all the mul-

TABLE III. Auger and x-ray transition probabilities (in multiples of 10^{-4} a.u.) to the K shell for initial $(1s)^1(2s)^0(2p)^n$ configurations of Ne, multiplet fluorescence yields $\omega(LS)$, and effective configuration fluorescence yields $\bar{\omega}(n)$ (calculated for statistical population).

n	Multiplet[a]	Auger rate K-$L_{23}L_{23}$	X-ray rate	$\omega(LS)$	$\bar{\omega}(n)$
6	^2S	82.125	1.806	0.0215	0.0215
5	^1P	64.312	2.672	0.0399	0.0253
	^3P	64.312	1.336	0.0204	
4	^2S	45.973	1.478	0.0311	0.0325
	^2P	37.677	2.956	0.0727	
	^2D	58.624	1.478	0.0246	
	^4P	37.677	0.739	0.0192	
3	$^3S'$	0.0644	3.254	0.981	0.106
	$^5S'$	0.004 02	0.000 123	0.0297	
	^1P	26.658	2.444	0.0840	
	^3P	26.658	0.815	0.0297	
	^1D	36.423	2.444	0.0629	
	^3D	36.423	0.815	0.0219	
2	$^3P'_{3/2}$	0.118	2.667	0.958	0.238
	$^3P'_{1/2}$	0.008 71	2.667	0.997	
	^2S	11.160	0.889	0.0738	
	^2D	27.813	0.889	0.0310	
	$^4P'_{5/2}$	0.008 28	0.000 265	0.0310	
	$^4P'_{3/2}$	0.001 25	0.000 172	0.121	
	$^4P'_{1/2}$	0.002 32	0.000 245	0.0957	

[a] Primes indicate inclusion of spin-orbit interaction mixing.

tiplet states and much larger than the respective radiative widths, $\Gamma_A(LS,n) >> \Gamma_R(LS,n)$. Equation (29) then approximately agrees with Eq. (3):

$$\bar{\omega}(n) \cong \frac{\sum_{L,S}(2L+1)(2S+1)[\Gamma_R(LS,n)/\Gamma_A(LS,n)]}{\sum_{L,S}(2L+1)(2S+1)[\Gamma_R(LS,n)/\Gamma_A(LS,n)+1]}$$

$$\cong \frac{\sum_{L,S}(2L+1)(2S+1)\omega(LS,n)}{\sum_{L,S}(2L+1)(2S+1)}. \qquad (30)$$

For the higher-charge states, the differences between results from Eqs. (3) and (29) grow,

TABLE IV. Spin-orbit parameters ζ_{2p} and Slater integrals F^k and G^k for $(1s)^1(2s)^m(2p)^n$ electron configurations of Ne. (All quantities are in eV.)

m	n	ζ_{2p}	$F^2(2p,2p)$	$G^1(1s,2p)$	$G^1(2s,2p)$	$G^0(1s,2s)$
1	3	0.163 54	18.229	8.6349	20.952	4.2031
1	2	0.182 23	19.225	9.3920	21.596	4.4840
1	1	0.199 17	20.220	10.128	22.275	4.7863
0	3	0.177 84	19.036	9.1994		
0	2	0.194 59	20.086	9.9487		

TABLE V. Possible configurations, their fluorescence yields $\bar{\omega}(n)$ and statistical weights, for Ne charge states KL^i, and average fluorescence yields $\bar{\omega}^i$ for each charge state, calculated for statistical population.

Charge state	Configuration	$\bar{\omega}(n)$	Weight	$\bar{\omega}^i$
KL^0	$(1s)^1(2s)^2(2p)^6$	0.0159	1	0.0159
KL^1	$(1s)^1(2s)^2(2p)^5$	0.0168	12	0.0175
	$(1s)^1(2s)^1(2p)^6$	0.0196	4	
KL^2	$(1s)^1(2s)^2(2p)^4$	0.0185	30	0.0199
	$(1s)^1(2s)^1(2p)^5$	0.0215	24	
	$(1s)^1(2s)^0(2p)^6$	0.0215	2	
KL^3	$(1s)^1(2s)^2(2p)^3$	0.0229	40	0.0248
	$(1s)^1(2s)^1(2p)^4$	0.0260	60	
	$(1s)^1(2s)^0(2p)^5$	0.0253	12	
KL^4	$(1s)^1(2s)^2(2p)^2$	0.0272	30	0.0390
	$(1s)^1(2s)^1(2p)^3$	0.0459	80	
	$(1s)^1(2s)^0(2p)^4$	0.0325	30	
KL^5	$(1s)^1(2s)^2(2p)^1$	0.0239	12	0.0862
	$(1s)^1(2s)^1(2p)^2$	0.0855	60	
	$(1s)^1(2s)^0(2p)^3$	0.106	40	
KL^6	$(1s)^1(2s)^2(2p)^0$	0	2	0.229
	$(1s)^1(2s)^1(2p)^1$	0.237	24	
	$(1s)^1(2s)^0(2p)^2$	0.238	30	

reaching a factor of 3 for the $(1s)^1(2p)^2$ and $(1s)^1(2s)^1(2p)^1$ configurations. In these higher charge states, the Auger channel is closed for some of the multiplets, in LS coupling, due to selection rules. For such multiplets, the fluorescence yields are very large. This effect is not taken into account when average yields are computed through Eq. (29).

The metastable state $^4P_{5/2}$ in the $(1s)^1(2s)^1(2p)^1$ configuration has both x-ray and Auger channels closed. The $M2$ x-ray decay rate and the Auger transition probability for this state have been determined through a Dirac-Hartree-Fock calculation by Cheng, Lin, and Johnson.[21] Their results are included in Table II.

The question can well be asked whether configuration mixing affects the present results significantly. In particular, the ^3S state of the $1s(2p)^3$ configuration and the ^2P state of the $1s(2p)^2$ configuration have very high fluorescence yields because for these states the Auger channel is closed in LS coupling. Conceivably, these configurations might draw Auger strength from other configurations, due to configuration mixing, with a consequent large reduction in multiplet fluorescence yields. This, however, is not the case, as indicated by the following argument. For $1s(2p)^3\,^3S$, the nearby configurations with which mixing might occur are $1s(2p)^23p\,^3S$, $1s(2p)^24p\,^3S$, and $1s2p(3p)^2\,^3S$. For

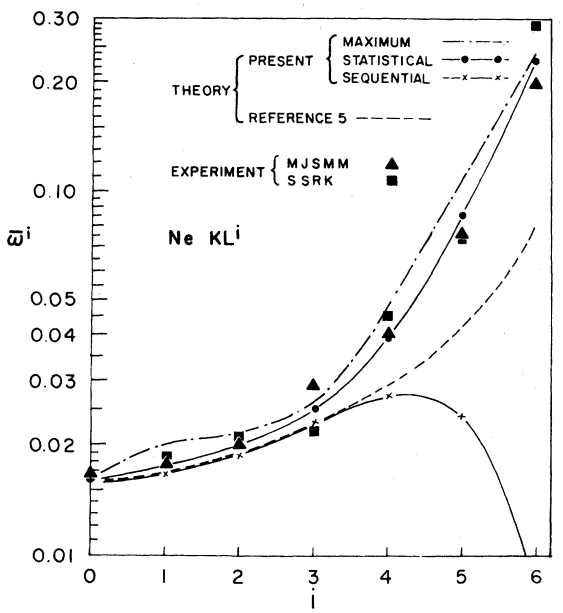

FIG. 1. Theoretical K-shell fluorescence yields for Ne KL^i charge states, calculated for statistical distribution of vacancy states and for sequential stripping; the maximum possible fluorescence yield for each charge state is also indicated. For comparison, theoretical results from Ref. 5 and measured fluorescence yields from Refs. 22 (MJSMM) and 23 (SSRK) are shown; experimental values have been adjusted for a $^4P/KL^6$ ratio of 0.40.

these latter three configurations, the Auger transition $^3S \rightarrow (1s)^2np\,^2P$ ($n=2, 3, 4$) is forbidden, because the selection rule $\Delta L = 0$ requires that the continuum electron be emitted in a p state, while parity conservation requires that the continuum electron be in an even state. Similar reasoning shows that the $1s(2p)^2\,^2P$ state cannot pick up Auger strength from mixing with the nearby $1s2p3p\,^2P$ and $1s(3p)^2\,^2P$ states.

Charge-state fluorescence yields $\bar{\omega}^i$ are compared in Fig. 1 with those from Ref. 5, and with experimental results of Matthews *et al.*[22] and of Stolterfoht *et al.*[23] Details of the comparison have been discussed elsewhere.[6] The original semiempirical results of Refs. 22 and 23 are at variance because the respective authors used different correction factors in an attempt to account for the overlap of the KL^5 peak in the measured x-ray spectrum with the ^4P line from the KL^6 state. The points indicated in Fig. 1 have been adjusted[6] using our theoretical ratio between quartet and doublet x-ray decay rates, which is 0.40. The two sets of semiempirical fluorescence yields then become consistent with each other and with the present theoretical yields computed on the basis of statistical distribution of initial states. Experimental results in Fig. 1 pertain to the bombardment of Ne with 30-MeV O^{5+} ions.[6,22,23] On the other hand, results from the bombardment of Ne with O^{8+} and Cl^{13+} ions, when analyzed with the present theoretical transition probabilities, show that in these latter cases nonstatistical vacancy distributions are produced.[24]

Note added in proof. A paper by C. P. Bhalla [Phys. Rev. A 12, 122 (1975)] has been called to our attention. Results from the two articles are in general agreement, even though the formalisms employed to compute Auger rates are quite different.

ACKOWLEDGMENT

The authors wish to thank D. L. Matthews of the Lawrence Livermore Laboratory for many helpful discussions.

†Work supported in part by the U. S. Army Research Office-Durham (Grant DAHC04-75-G-0021) and by the National Aeronautics and Space Administration (Grant NGR 38-003-036).

[1]M. H. Chen and B. Crasemann, Phys. Fennica 9, S1, 250 (1974).
[2]M. H. Chen and B. Crasemann, Phys. Rev. A 10, 2232 (1974).
[3]F. P. Larkins, J. Phys. B 5, L29 (1971).
[4]R. J. Fortner, R. C. Der, T. M. Kavanagh, and J. D. Garcia, J. Phys. B 5, L73 (1972).
[5]C. P. Bhalla, N. O. Folland, and M. A. Heins, Phys. Rev. A 8, 649 (1973).
[6]M. H. Chen, B. Crasemann, and D. L. Matthews, Phys. Rev. Lett. 34, 1309 (1975).
[7]E. J. McGuire, Phys. Rev. A 10, 13 (1974).
[8]E. J. McGuire, Phys. Rev. A 11, 1889 (1975).
[9]E. J. McGuire, in *Atomic Inner-Shell Processes*, edited by B. Crasemann (Academic, New York, 1975), Vol. 1, p. 293.
[10]V. O. Kostroun, M. H. Chen, and B. Crasemann, Phys. Rev. A 3, 533 (1971).
[11]J. C. Slater, *Quantum Theory of Atomic Structure* (McGraw-Hill, New York, 1960), Vol. 2.
[12]B. W. Shore and D. H. Menzel, *Principles of Atomic Spectra* (Wiley, New York, 1968); Astrophys. J. Suppl. Ser. 12, 187 (1965).
[13]E. U. Condon and G. H. Shortley, *The Theory of Atomic Spectra* (Cambridge U. P., Cambridge, England, 1953).
[14]B. G. Wybourne, *Spectroscopic Properties of Rare Earths* (Wiley, New York, 1965).
[15]F. Herman and S. Skillman, *Atomic Structure Calculations* (Prentice-Hall, Englewood Cliffs, N. J., 1963).
[16]L. I Yin, I. Adler, T. Tsang, M. H. Chen, and B. Crasemann, Phys. Rev. A 9, 1070 (1974).
[17]K. Schwarz, Phys. Rev. B 5, 2466 (1972).

[18]F. P. Larkins, J. Phys. B 4, 14 (1971).
[19]D. L. Matthews (private communication).
[20]E. J. McGuire, Phys. Rev. A 11, 10 (1975).
[21]K. Cheng, C. Lin, and W. R. Johnson, Phys. Lett. 48A, 437 (1974).
[22]D. L. Matthews, B. M. Johnson, L. E. Smith, J. J. Mackey, and C. F. Moore, Phys. Lett. 48A, 93 (1974). For revised results see C. F. Moore and D. L. Matthews, in *Proceedings of the Third Conference on the Applications of Small Accelerators*, edited by J. L. Duggan (North Texas State University, Denton, Tex., 1974); and D. L. Matthews, B. M. Johnson, G. W. Hoffmann, and C. F. Moore, Phys. Lett. 49A, 195 (1974).
[23]N. Stolterfoht, D. Schneider, P. Richard, and R. L. Kauffman, Phys. Rev. Lett. 33, 1418 (1974).
[24]D. L. Matthews, R. J. Fortner, M. H. Chen, and B. Crasemann, *Electronic and Atomic Collisions, Abstracts of Papers of the Ninth International Conference on the Physics of Electronic and Atomic Collisions*, edited by J.S. Risley and R. Geballe (University of Washington Press, 1975), Vol. 2, p. 941.